

# *Evidence that Inositol-1,4,5-trisphosphate-3-kinase and Inositol-1,3,4,5-tetrakisphosphate are negative regulators of platelet function*

Article

Published Version

Creative Commons: Attribution 4.0 (CC-BY)

Open Access

Authi, K. S., Khan, S., Gibbins, J. M. ORCID: <https://orcid.org/0000-0002-0372-5352> and Brain, S. D. (2024) Evidence that Inositol-1,4,5-trisphosphate-3-kinase and Inositol-1,3,4,5-tetrakisphosphate are negative regulators of platelet function. *Research and Practice in Thrombosis and Haemostasis*, 8 (1). 102326. ISSN 2475-0379 doi: <https://doi.org/10.1016/j.rpth.2024.102326> Available at <https://centaur.reading.ac.uk/114606/>

It is advisable to refer to the publisher's version if you intend to cite from the work. See [Guidance on citing](#).

To link to this article DOI: <http://dx.doi.org/10.1016/j.rpth.2024.102326>

Publisher: Elsevier

All outputs in CentAUR are protected by Intellectual Property Rights law, including copyright law. Copyright and IPR is retained by the creators or other copyright holders. Terms and conditions for use of this material are defined in the [End User Agreement](#).

[www.reading.ac.uk/centaur](http://www.reading.ac.uk/centaur)

**CentAUR**

Central Archive at the University of Reading

Reading's research outputs online

**ORIGINAL ARTICLE**

# Evidence that inositol 1,4,5-trisphosphate 3-kinase and inositol 1,3,4,5-tetrakisphosphate are negative regulators of platelet function

Kalwant S. Authi<sup>1</sup> | Sabeeya Khan<sup>2</sup> | Jonathan M. Gibbins<sup>2</sup>  | Susan D. Brain<sup>1</sup>

<sup>1</sup>School of Cardiovascular and Metabolic Medicine and Sciences, BHF Centre for Research Excellence, London, UK

<sup>2</sup>Institute for Cardiovascular and Metabolic Research, School of Biological Sciences, University of Reading, Reading, UK

**Correspondence**

Kalwant S. Authi, School of Cardiovascular and Metabolic Medicine and Sciences, BHF Centre for Research Excellence, Room 3.12 Franklin Wilkins Building, 150 Stamford Street, London SE1 9NH, UK.  
Email: [kalwant.authi@kcl.ac.uk](mailto:kalwant.authi@kcl.ac.uk)

**Handling Editor:** Dr Yotis Senis

**Abstract**

**Background:** Inositol 1,3,4,5-tetrakisphosphate (IP<sub>4</sub>) is formed from inositol 1,4,5-trisphosphate (IP<sub>3</sub>) by IP<sub>3</sub> 3-kinase (ITPK) in most cells. Its function is unknown but has been suggested to be involved in Ca<sup>2+</sup> entry, IP<sub>3</sub> regulation, and phosphoinositide 3-kinase antagonism.

**Objectives:** To better elucidate a function for IP<sub>4</sub>, we tested a specific inhibitor of ITPK (GNF362) on platelets, the effects of IP<sub>4</sub> directly in permeabilized platelets and its effect on phosphatidylinositol 3,4,5-trisphosphate (PIP<sub>3</sub>) binding to pleckstrin-homology (PH) domain-containing proteins in platelets.

**Methods:** Human platelets were utilized in whole blood for thrombus formation, in platelet-rich plasma and washed suspensions for aggregation, and for Ca<sup>2+</sup> studies, or resuspended in high K<sup>+</sup> and low Na<sup>+</sup> buffers for permeabilization experiments. Phosphorylation of AKT-Ser<sup>473</sup> and Rap1-GTP formation were measured by Western blotting and PIP<sub>3</sub> binding using PIP<sub>3</sub> beads.

**Results:** GNF362-enhanced platelet aggregation stimulated by low concentrations of ADP, collagen, thrombin, U46619, and thrombus formation in collagen-coated capillaries. GNF362 induced a transient elevation of Ca<sup>2+</sup> concentration, elevated basal levels of IP<sub>3</sub>, and enhanced the peak height of Ca<sup>2+</sup> elevated by agonists. In permeabilized platelets, IP<sub>4</sub> inhibited GTPγS induced formation of AKT-Ser<sup>473</sup> phosphorylation and platelet aggregation. IP<sub>4</sub> reduced GTPγS-stimulated Rap1-GTP levels and potentially reduced extraction of RASA3 and BTK by PIP<sub>3</sub> beads.

**Conclusion:** ITPK and IP<sub>4</sub> are negative regulators of platelet function. IP<sub>4</sub> regulation of PH domain-containing proteins may represent a pathway by which platelet activation may be controlled during thrombosis.

**KEYWORDS**

inositol 1,3,4,5-tetrakisphosphate, inositol 1,4,5-trisphosphate 3-kinase, platelet activation, phosphoinositide 3-kinase, phosphatidylinositol 3,4,5-trisphosphate

## Essentials

- The function of inositol 1,3,4,5-tetrakisphosphate (IP<sub>4</sub>) in platelets is not known.
- An inhibitor of inositol 1,4,5-trisphosphate 3-kinase (ITPK), GNF362, and IP<sub>4</sub> were tested.
- GNF362 increased platelet activation and IP<sub>4</sub> inhibited platelet responses in permeabilized cells.
- ITPK and IP<sub>4</sub> are negative regulators of platelet activation.

## 1 | INTRODUCTION

Platelet function is very important in many cardiovascular functions and pathologies such as hemostasis, thrombosis, inflammation, and in the progression of cancer. Current antiplatelet therapy has proven benefit in reducing adverse cardiovascular events but can also lead to increased bleeding. There is thus a need for therapy that is effective but also has fewer side effects. There is increasing laboratory evidence that targeting the phosphoinositide pathways that are linked to increased intracellular Ca<sup>2+</sup> can inhibit experimental thrombosis and has minor effects on hemostasis [1–5].

Intracellular Ca<sup>2+</sup> increase is an essential part of platelet activation and occurs when G-protein-linked receptor agonists (such as thrombin, thromboxane A<sub>2</sub>, and ADP) and adhesion receptor agonists (such as collagen and CLEC2) stimulate phospholipase C (PLC) to convert phosphatidylinositol 4,5-bisphosphate to produce inositol 1,4,5-trisphosphate (IP<sub>3</sub>) and 1,2-diaclyglycerol (DAG). IP<sub>3</sub> releases Ca<sup>2+</sup> from intracellular stores via the IP<sub>3</sub> receptors (IP<sub>3</sub>R) that then leads to Ca<sup>2+</sup> entry via store-operated Ca<sup>2+</sup> entry, and DAG stimulates protein kinase C [6]. IP<sub>3</sub> is converted to inositol 1,3,4,5-tetrakisphosphate (IP<sub>4</sub>) by the action of IP<sub>3</sub> 3-kinase (ITPK) or degraded to inositol 1,4-diphosphate (IP<sub>2</sub>) by IP<sub>3</sub> 5-phosphatase. IP<sub>4</sub> can be broken down to inositol 1,3,4-trisphosphate and eventually to inositol or it can serve as a precursor for the synthesis of higher inositol phosphates such as IP<sub>5</sub> and IP<sub>6</sub> [7–9]. Platelet activation also leads to the generation of phosphatidylinositol 3,4,5-trisphosphate (PIP<sub>3</sub>) from phosphatidylinositol 4,5-bisphosphate by the activation of phosphoinositide 3-kinase (PI3K). Newly generated PIP<sub>3</sub> acts to recruit signaling proteins that have pleckstrin-homology (PH) domains to the membrane where their manipulation leads to the stimulation of downstream effectors such as protein kinase B (PKB—also known as AKT), Bruton's tyrosine kinase (BTK), the Ras- and Rap GTP-activating protein RASA3, and many others [10]. In platelet biology, it is generally accepted that sustained activation resulting in aggregation, secretion of granule contents, and procoagulant expression requires all the activation pathways to be maximally operative in a complex and highly coordinated manner. The fine regulation of these pathways is still under investigation and may lead to the development of newer targets for therapeutic development.

The conversion of IP<sub>3</sub> to IP<sub>4</sub> and possible functions of IP<sub>4</sub> have attracted considerable investigations and debate. As the formation of IP<sub>4</sub> requires ATP and the ITPK enzymes are Ca<sup>2+</sup>-stimulated [9,11], many investigators sought specific functions for IP<sub>4</sub>. Initially, a role for IP<sub>4</sub> in Ca<sup>2+</sup> entry was postulated [12], reported to open Ca<sup>2+</sup>

entry channels in endothelial cells [13], to enhance IP<sub>3</sub>-promoted Ca<sup>2+</sup>-activated K<sup>+</sup> currents [14] and inhibition of IP<sub>3</sub> 5-phosphatase [15], and to promote IP<sub>3</sub>-dependent Ca<sup>2+</sup> release from IP<sub>3</sub>R present close to or in the plasma membrane [16]. However, in contrast, IP<sub>4</sub> has also been suggested to inhibit Ca<sup>2+</sup> entry channels [17]. Since the formation of IP<sub>4</sub> from IP<sub>3</sub> would lead to a decrease in IP<sub>3</sub> levels, this may in turn limit IP<sub>3</sub>-induced Ca<sup>2+</sup> release from stores. Structurally, IP<sub>4</sub> has the same head group as PIP<sub>3</sub> and is able to potently bind to PH domains such as that found in Bruton's tyrosine kinase (BTK) [18] and the protein RASA3 [19] (originally called GAP1-<sup>IP4BP</sup>). However as PIP<sub>3</sub> contains the diacylglycerol moiety, it remains in the plasma membrane, whereas IP<sub>4</sub> is soluble and thus may function in the cytosolic phase where the majority of these proteins reside. IP<sub>4</sub> may thus either co-activate or oppose PIP<sub>3</sub> signaling. In natural killer cells, IP<sub>4</sub> has been reported to limit interferon gamma secretion and granule exocytosis in part by inhibiting PIP<sub>3</sub>-dependent AKT activation [20]. Similarly, in hematopoietic stem cells, the absence of ITPKB isoform upregulated activation of these cells via the PI3K pathway but impaired their longevity [21]. This suggests that IP<sub>4</sub> may act to regulate the PI-3K pathway and, in its absence, PIP<sub>3</sub>-dependent activation would be enhanced.

In platelets, there have been limited studies exploring IP<sub>4</sub> function. O'Rourke et al. reported that IP<sub>4</sub> mobilizes Ca<sup>2+</sup> from isolated platelet membranes loaded with Ca<sup>2+</sup> oxalate [22]. In highly purified platelet plasma membranes, this group has shown that IP<sub>4</sub> may mobilize Ca<sup>2+</sup> through a distinct mechanism from that mediated by IP<sub>3</sub> [23]. Furthermore, cell-permeable PIP<sub>3</sub> analogs such as DiC8-PIP<sub>3</sub> induced transient Ca<sup>2+</sup> elevation in washed platelets [24] and there is evidence that PIP<sub>3</sub> may bind to the nonspecific Ca<sup>2+</sup> entry channel TRPC6 [25]. Thus far, no studies have examined any interaction of IP<sub>4</sub> with the PI3K-AKT pathway in platelets. In light of the potential opposing and controversial roles postulated for IP<sub>4</sub>, this study has re-examined functions for IP<sub>4</sub> via 2 approaches. We describe the effect of GNF362 [26], a recently described inhibitor of ITPK, on platelet aggregation; on Ca<sup>2+</sup> mobilization in isolated platelets; and on thrombus formation in collagen-coated capillaries. We examined in a permeabilized platelet model the effects of introducing IP<sub>4</sub> into the cytosol on aggregation mediated by the nonhydrolyzable analog of GTP (GTP<sub>γ</sub>S), on AKT phosphorylation, Rap1-GTP formation, and in lysates, the binding of PIP<sub>3</sub> on beads to the PH domain-containing proteins from platelets. Our results suggest that inhibiting ITPK by GNF362 results in the enhancement of platelet activation by the main platelet agonists and increases thrombus formation in collagen-coated capillaries, and in permeabilized cell systems, IP<sub>4</sub> inhibits AKT

phosphorylation, Rap1-GTP formation, and platelet aggregation and displaces PIP<sub>3</sub> from PH domain-containing proteins such as RASA3 and BTK. Our studies suggest important negative regulatory roles for ITPK and IP<sub>4</sub> in platelet function.

## 2 | METHODS

### 2.1 | Reagents

DiC8-PIP<sub>3</sub>, In(1,3,4,5)P<sub>4</sub>, In(1,4,5)P<sub>3</sub> (IP<sub>3</sub>), and GNF362 were obtained from Cambridge Bioscience Ltd. Fura2-AM was obtained from Thermo Fisher Scientific, and U46619 was obtained from Tocris. The phospho-AKT antibody recognizing phospho-Ser<sup>473</sup> (clone 11E61) was obtained from Upstate. The pan-AKT antibody (C67E7) recognizing Akt1, Akt2, and Akt3 proteins was obtained from Cell Signaling Technology. Goat antimouse antibody linked to horseradish peroxidase (HRP) and Goat antirabbit-HRP were purchased from Millipore. Antibodies to GAP1(IP4BP/RASA3), ITPKB, ITPKA, and BTK were purchased from (Santa Cruz Biotechnology Inc). The anti-Rap1(A+B) and IP<sub>3</sub>-ELISA kit was purchased from Abcam Ltd. GTP $\gamma$ S and RalGDS-RBD beads were obtained from Abcam Ltd. PI(3,4,5)P<sub>3</sub> PIP beads (PIP<sub>3</sub> beads) were obtained from Echelon Biosciences (via 2B Scientific). Vena8 Cellix microfluidic chip channels were obtained from Cellix Ltd.

### 2.2 | Preparation of human platelets for studies in platelet-rich plasma or washed cells with Fura-2AM loading

Blood was taken from human donors after written consent (with approval from King's College London and University of Reading Research Ethics Committees) into 0.1 volume of 3.2 % trisodium citrate. Platelet-rich plasma (PRP) was isolated after centrifugation of the blood at 200 $\times$  g for 20 minutes. In studies measuring intracellular Ca<sup>2+</sup> levels, the platelets were labeled with Fura-2AM in PRP at 37 °C with 3  $\mu$ M Fura-2AM for 1 hour in the dark. The PRP was then cooled to room temperature and acidified to pH 6.5 with 0.3 M citric acid, and EDTA was added to a final concentration of 3 mM and then centrifuged at 1200 $\times$  g for 20 minutes. The platelet pellet was washed in an EDTA-citrate washing buffer comprising 36 mM citric acid, 1 mM EDTA, 5 mM glucose, 5 mM KCl, 103 mM NaCl (pH: 6.5), and 100 nM PGE<sub>1</sub>. After centrifugation, the platelet pellet was resuspended at 1 to 1.5  $\times$  10<sup>8</sup> cells/mL in a HEPES Tyrode buffer comprising 10 mM HEPES, 140 mM NaCl, 5 mM KCl, 1 mM MgCl, 5 mM glucose, 0.42 mM NaH<sub>2</sub>PO<sub>4</sub>, and 12 mM NaHCO<sub>3</sub> (pH: 7.35). For Ca<sup>2+</sup> studies, 2 mL suspensions were used at 37 °C with continuous stirring using a purpose built spectrofluorimeter (Cairns Research Ltd). Continuous fluorescence measurements were made with excitation at 340 and 380 nm and emission at 510 nm. [Ca<sup>2+</sup>]<sub>i</sub> is reported as the 340 nm/380 nm ratio (R<sub>340/380</sub>), where indicated ratio values were converted to nM Ca<sup>2+</sup> using the equation of Grynkiewicz et al. [27] as described by Sage [28].

### 2.3 | Preparation of platelets for aggregation, saponin permeabilization, phospho-AKT-Ser<sup>473</sup> analysis, and Rap1-GTP determination

Washed platelets were isolated as described above (without Fura2 loading) and were resuspended in the HEPES Tyrode's medium at 2.5  $\times$  10<sup>8</sup> cells/mL. Incubations were carried out in aggregation cuvettes using a Biodata PAP4 aggregometer using 400- $\mu$ L suspensions at 37 °C with 1 mM Ca<sup>2+</sup> and stirring. Reagents were added for the times stated in the Results section and aggregations were measured for 5 minutes. For saponin permeabilization studies, the washed platelets were resuspended in a buffer containing 140 mM KCl, 5 mM glucose, 1 mM MgCl<sub>2</sub>, 0.42 mM NaH<sub>2</sub>PO<sub>4</sub>, 6 mM NaHCO<sub>3</sub>, and 10 mM HEPES made up in HPLC grade water (Sigma-Aldrich) and buffered to pH 7.4. For Rap1 and AKT-phosphorylation studies, the cell count was adjusted to 4  $\times$  10<sup>8</sup>/mL. In typical experiments, 400- $\mu$ L cells were equilibrated at 37 °C for 3 minutes, and saponin (13 to 15  $\mu$ g/mL) was added to give an increase of light transmission (aggregation) of between 10% and 20% over an 8 minute period. GTP $\gamma$ S (at either 1 or 2 minutes after saponin addition) or other reagents were added as described in the Figure legends. For Rap1-GTP analysis, the incubations were stopped with ice cold equal volume 2 $\times$  NP40 lysis buffer containing 100 mM Tris, 400 mM NaCl, 5 mM MgCl<sub>2</sub>, 2% NP40, 20% glycerol, 1% sodium deoxycholate, 2 mM PMSF, 20  $\mu$ M leupeptin, 0.4 U/mL aprotinin, 2 mM sodium vanadate, and 50 mM NaF (pH: 7.4). Incubations were kept on ice for 20 minutes and then centrifuged at 13,000 $\times$  g for 10 minutes at 4 °C. Then, aliquots of the supernatants were set aside, 2 $\times$  Laemmli buffer was added, and they were heated for 5 minutes at 97 °C for total protein inputs and phospho-AKT-Ser<sup>473</sup> analysis by Western blotting. Remaining supernatants were used for Rap1-GTP pull-down analysis by adding 15- $\mu$ g RalGDS-RBD beads and incubated for 1 hour with rotation at 4 °C, followed by centrifugation at 14,000 $\times$  g at 4 °C for 20 seconds. The pellets were washed 3 times with 1 $\times$  NP40 lysis buffer containing inhibitors, finally resuspended in 2 $\times$  Laemmli buffer, and heated for 5 minutes at 96 °C before Western blotting analysis.

Western blotting was carried out using 10% sodium dodecyl-sulfate-polyacrylamide gel electrophoresis gels, then transferred to polyvinylidene difluoride membranes, and blocked overnight with 5% BSA in TBS-Tween (20 mM Tris [pH: 7.4], 150 mM NaCl, 0.1% Tween). The polyvinylidene difluoride membranes were washed 2 times in TBS-Tween followed by incubation with primary antibody (eg, phospho-AKT-Ser<sup>473</sup> [at 1/400]) or AKT (pan) antibody at a dilution of 1/1000 in TBS-Tween for 2 hours at room temperature. After 4 washes with TBS-Tween, the membranes were incubated with an appropriate second antibody (eg, goat antimouse [usually 1/5000]) conjugated to HRP in TBS-Tween for 1 hour, followed by 4 washes and detection using chemiluminescence reagents (Thermo Fisher). Images of bands were scanned and analyzed with densitometry using ImageJ. Significance was determined using *t*-test analyzed with GraphPad Prism software. Antibodies used for Western blots in this study with their dilutions included Rap1(A+B) 1/1000; RASA3 1/200, BTK 1/400, ITPKA, and ITPKB 1/200.

IP<sub>3</sub> levels were estimated using an IP<sub>3</sub>-ELISA kit (Abcam). Platelets were resuspended at  $4 \times 10^8$  cells/mL, incubated at  $37 \text{ }^\circ\text{C} \pm 10 \text{ }^\circ\text{C}$   $\mu\text{M}$  GNF362 for 1 minute in aggregometer cuvettes with stirring, and stopped with cold 5 mM EDTA/1  $\mu\text{M}$  indomethacin, followed by 3 cycles of freeze–thaw and centrifugation at  $13,000 \times g$  for 10 minutes at  $4 \text{ }^\circ\text{C}$ . Aliquots of the supernatants were analyzed by the IP<sub>3</sub>-ELISA kit according to the manufacturer's protocol. Experiments involving protein pull down with PIP<sub>3</sub> beads were carried out as follows. After washing in EDTA-citrate buffer, the platelet pellets were lysed at an equivalent platelet count of  $1 \times 10^9$  /mL with PIP<sub>3</sub> lysing buffer comprising 20 mM Hepes (pH: 7.4), 120 mM NaCl, 0.5% NP40, 5 mM EDTA, 5 mM EGTA, 5 mM  $\beta$ -glycerophosphate, 10 mM NaF, 1 mM sodium vanadate, 2 mM PMSF, 20  $\mu\text{M}$  leupeptin, and 0.4 U/mL aprotinin. After 20 minutes at  $4 \text{ }^\circ\text{C}$ , the suspensions were centrifuged at  $16,000 \times g$  for 10 minutes and the supernatants were used for the extraction of PIP<sub>3</sub> beads. Aliquots (0.4 mL) were incubated with either vehicle (water/dimethyl sulfoxide) or 40  $\mu\text{M}$  DiC8-PIP<sub>3</sub>, or 0.1 to 80  $\mu\text{M}$  IP<sub>4</sub>, and incubated at  $4 \text{ }^\circ\text{C}$  for 30 minutes, followed by addition of either control beads or PIP<sub>3</sub> attached beads (35  $\mu\text{L}$  equivalent to a calculated concentration of 800 nM PIP<sub>3</sub>) for 90 minutes at  $4 \text{ }^\circ\text{C}$  with rotation. The suspensions were centrifuged at  $1000 \times g$  for 5 minutes at  $4 \text{ }^\circ\text{C}$  in an Eppendorf centrifuge, and the pellets were washed 3 times with lysis buffer and dissolved with 2 $\times$  Laemmli buffer for Western blotting analysis of the extracted proteins.

Thrombus formation on collagen-coated capillaries was carried out as described previously [29]. Briefly, whole blood was incubated with the fluorescent dye DiOC<sub>6</sub> (0.4  $\mu\text{g}/\text{mL}$ ) for 20 minutes in the dark at  $30 \text{ }^\circ\text{C}$ . Vena8 microfluidic chip channels (with dimensions [width  $\times$  height  $\times$  length] of  $0.04 \times 0.01 \times 2.8 \text{ cm}$ , respectively) were coated with 2  $\mu\text{L}$  of 0.1-mg/mL collagen for 1 hour at room temperature. Blood was incubated with either vehicle control (dimethyl sulfoxide) or GNF362 (10  $\mu\text{M}$ ) for 5 minutes prior to perfusion through the capillaries at a shear rate of  $1000 \text{ s}^{-1}$  for 5 minutes at  $30 \text{ }^\circ\text{C}$  while placed on the stage of a Nikon A1R laser confocal microscope. The formed thrombi were washed with Tyrode buffer and Z stack images were taken at 3 different areas of the channels. Image J was used to measure the volume of the thrombi.

All statistical analyses were carried out using GraphPad Prism software. Student's unpaired *t*-test was used to test for statistical significance.

## 3 | RESULTS

### 3.1 | The ITPK inhibitor GNF362 enhances aggregation of platelets induced by low concentrations of agonists

We first tested for the presence of ITPK isoforms expressed in human platelets using Western blotting. Figure 1A shows typical analysis from 2 different platelet preparations (out of 4) with distinct bands at expected sizes of  $\sim 45 \text{ kDa}$  and  $120 \text{ kDa}$  corresponding to ITPKA and ITPKB, respectively, suggesting the presence of both isoforms.

Currently, we do not have antibodies to ITPKC to test its presence. We then tested the inhibitor of ITPKs (GNF362) to examine if it affected platelet responses to the major platelet agonists. GNF362 has been shown to inhibit ITPKA, ITPKB, and ITPKC with a  $\text{IC}_{50}$  of about 20 nM, with total inhibition between 0.2 and 10  $\mu\text{M}$  [17,26]. The effects on ADP-(using 2-methyl-5-ADP [ADPS]) or collagen-induced aggregation were tested using PRP without any further addition of  $\text{Ca}^{2+}$ . Figure 1B, C shows that incubation of PRP with 10  $\mu\text{M}$  GNF362 alone had no noticeable effect on aggregation of platelets measured over a 10-minute period. However, when added 5 minutes prior to addition of low doses of ADPS (10, 20, and 50 nM), there was a marked enhancement of aggregation. The effects were statistically significant, measuring extents of aggregation at 5 minutes induced by 10 and 20 nM ADPS in the presence or absence of 10  $\mu\text{M}$  GNF362 ( $P = .03$  and  $P = .0001$  for 10 nM and 20 nM ADPS, respectively). At higher concentrations, no enhancement was observed. When collagen-mediated aggregation was studied, the presence of GNF362 again enhanced the aggregation to low concentrations of collagen with no significant effects at higher concentrations ( $P = .014$  and  $P = .008$  for 0.3 and 0.6  $\mu\text{g}/\text{mL}$  collagen, respectively; Figure 1D, E). Noticeably, with collagen, the lag time to shape change was decreased in the presence of GNF362. At 0.3- $\mu\text{g}/\text{mL}$  collagen, the lag time to peak of shape change was 2 minutes 5 seconds in the absence and 1 minute 23 seconds in the presence of GNF362 ( $P = .0023$ ), suggesting an enhancement in the rate of activation of this response in the presence of the ITPK inhibitor. With both collagen and ADP in PRP, GNF362 was effective at concentrations of  $>8 \text{ } \mu\text{M}$ , with lower concentrations showing little effect (Figure 1F).

Using washed platelets, we tested the effects of GNF362 on thrombin and the thromboxane mimetic U46619. Figure 2A, B shows that addition of 10  $\mu\text{M}$  GNF362 to washed platelets induced a decrease of light transmission, indicating a shape change response. This response was present in the presence or absence of 1 mM extracellular  $\text{Ca}^{2+}$ . Shape change responses were seen by concentrations of GNF362 of  $>2 \text{ } \mu\text{M}$  and within 30 seconds of addition. When tested against thrombin, GNF362 when added 5 minutes prior to agonist addition enhanced the aggregation seen at low concentrations of thrombin (eg, at 0.12-U/mL thrombin, extent of aggregation was  $18\% \pm 12\%$  in the absence and  $71.5\% \pm 2.5\%$  in the presence of 10  $\mu\text{M}$  GNF362;  $n = 6$ ,  $P = .0016$  [mean  $\pm$  SEM]) with no significant difference at concentrations of  $\geq 0.25 \text{ U}/\text{mL}$ . With washed platelets, GNF362 was effective at  $\geq 0.5 \text{ } \mu\text{M}$  (Figure 2D), suggesting that in PRP, it may bind to plasma proteins reducing its potency. Similar effects were seen with U46619 as the agonist. At 0.1  $\mu\text{M}$  U46619, 10  $\mu\text{M}$  GNF362 enhanced the aggregation from  $2\% \pm 3.3\%$  to  $65\% \pm 2.4\%$  (mean  $\pm$  SEM;  $n = 4$ ,  $P = .0001$ ). At  $>0.2 \text{ } \mu\text{M}$  U46619, there was no difference in the extent of aggregation seen with GNF362.

We have previously shown platelets labeled with the fluorescent dye DiOC<sub>6</sub> in whole blood and perfused through collagen-coated capillaries at arterial shear (of  $1000 \text{ s}^{-1}$ ) will adhere to the collagen and form thrombi, and this is affected by antibodies to GPIB and STIM1 [29]. We therefore tested if GNF362 would affect the size of thrombi formed in this system. Figure 2G, H shows that 10  $\mu\text{M}$

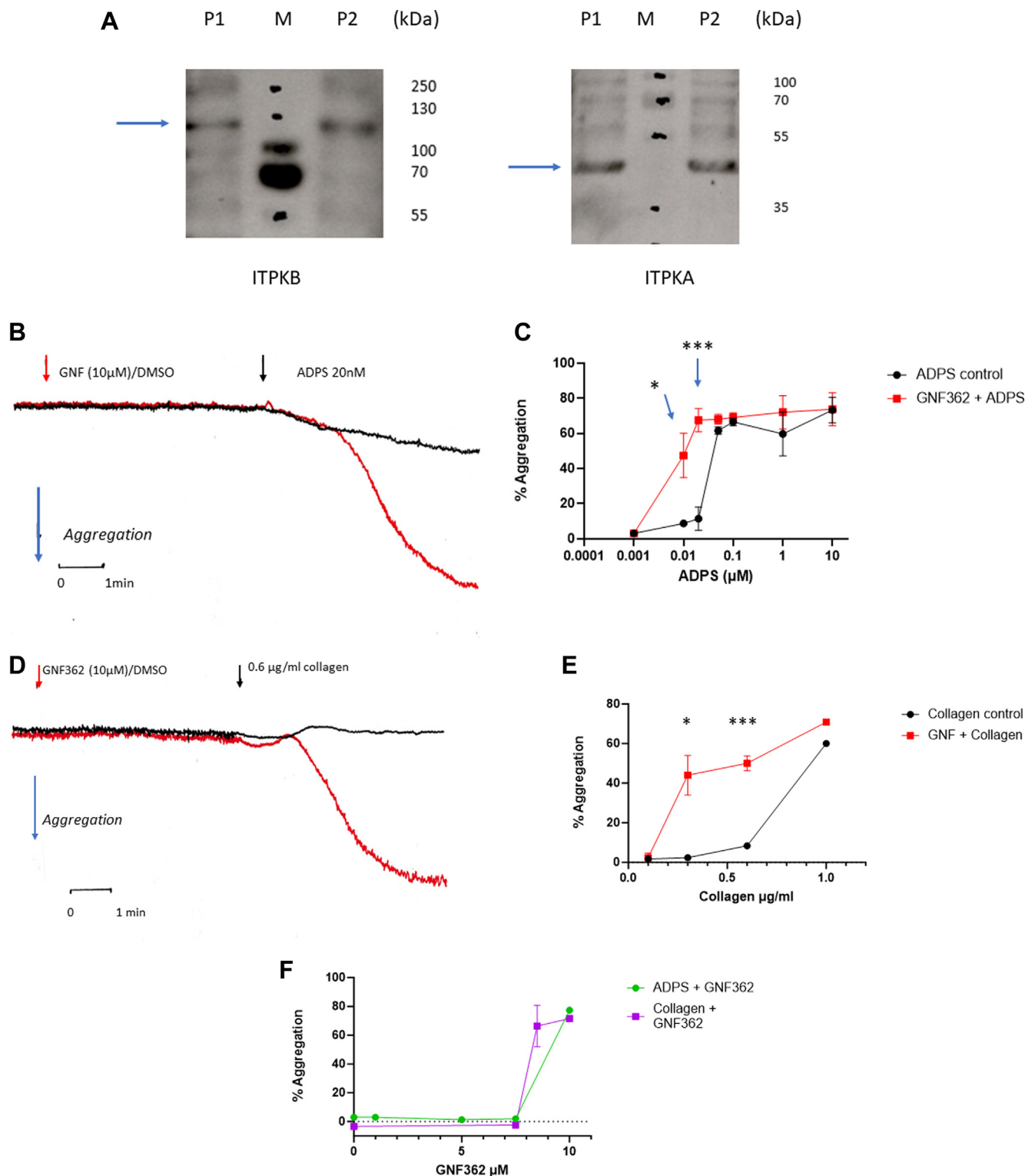


**FIGURE 1** Expression of ITPK isoforms in platelets and effects of GNF362 (GNF). (A) Western blots of platelet lysates P1 and P2 probed with ITPKA and ITPKB antibodies. Arrows point to identified bands for each isoform; M = molecular markers in kDa on the right of each blot. Typical of 4 different platelet preparations. (B, C) GNF362 enhances platelet aggregation to low doses of ADPS and (D, E) to collagen in PRP. (F) Dose-response relationship for GNF362 with ADPS and collagen in PRP. Aggregation traces shown are typical for 3 independent experiments with stirring at 37 °C. Red traces are incubations with GNF362, and black traces are those with vehicle DMSO. GNF362/DMSO was added 5 minutes prior to ADPS or collagen (at indicated concentrations) and recording measured for 5 minutes after agonist addition. Points are means  $\pm$  SEM ( $n = 3$ ). Student's unpaired  $t$ -test; (C) for 10 nM ADPS,  $P = .03$ , and for 20 nM ADPS,  $P = .0001$ . (E) For 0.3-μg/mL collagen,  $P = .014$ ; and for 0.6-μg/mL collagen,  $P = .0008$ . ADPS, 2-methyl-S-ADP; DMSO, dimethyl sulfoxide; ITPK, inositol 1,4,5-trisphosphate 3-kinase; PRP, platelet-rich plasma.

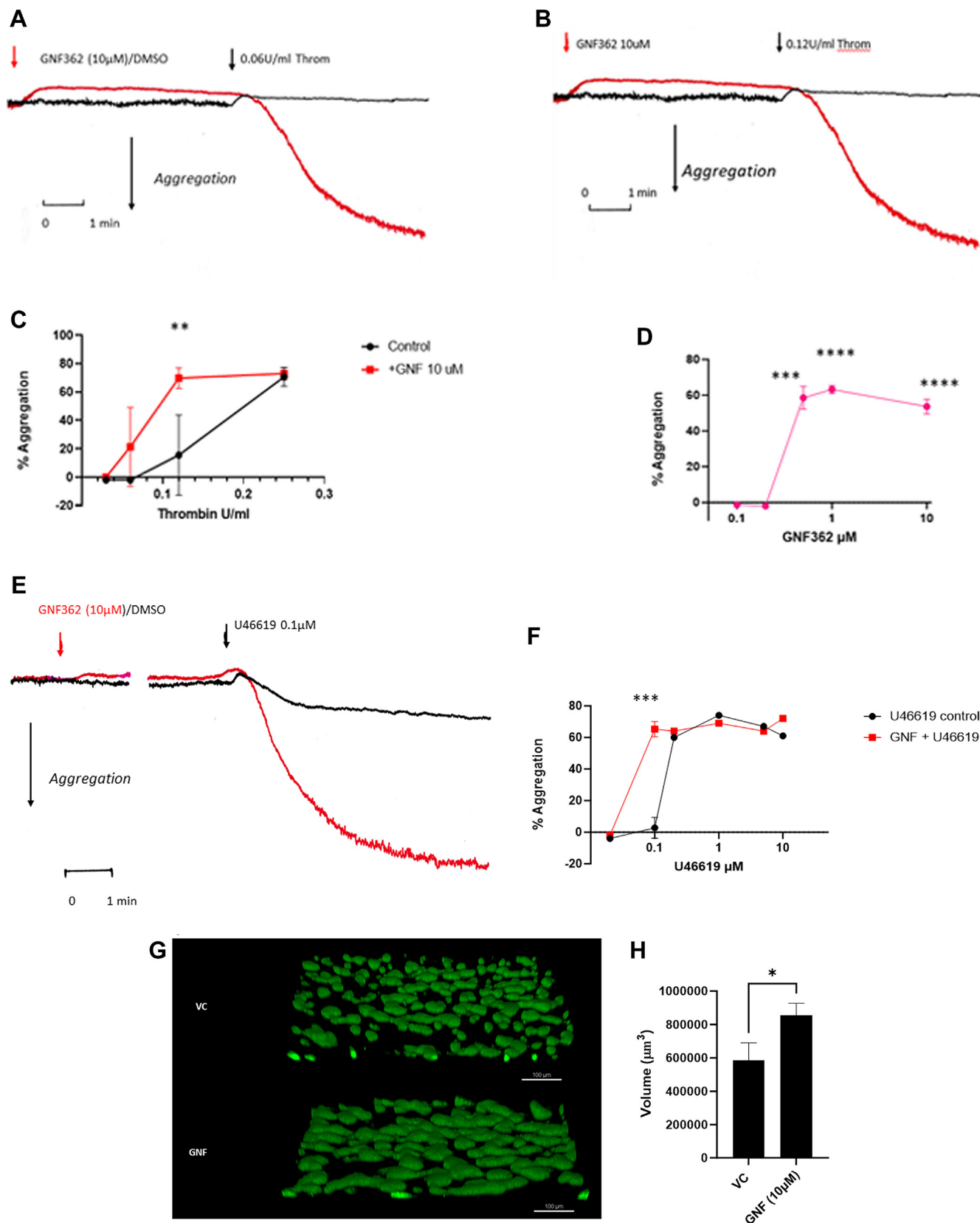


**FIGURE 2** GNF362 enhances aggregation responses to thrombin and U46619 in washed platelets, and thrombus formation in collagen-coated capillaries. (A–F) Washed platelets were incubated in aggregation tubes at 37 °C with stirring. GNF362 (red traces)/DMSO (black traces) was added at indicated times followed by agonist addition after 5 minutes. All incubations contained 1-mM Ca<sup>2+</sup>. Traces are typical of 6 independent experiments. All values are means  $\pm$  SEM, and *P* was calculated by Student's unpaired *t*-test; (C) at 0.12-U/mL thrombin, *P* = .0016.

GNF362 incubated for 5 minutes prior to flow significantly increased the volume of thrombi formed. This confirms that inhibition of ITPK by GNF362 enhances activation by all platelet agonists tested, suggesting that ITPK was an important regulator for both GPCR- and for ITAM-linked receptor agonists and thereby thrombus formation.

We then tested if the presence of GNF362 would lead to changes in  $\text{Ca}^{2+}$  levels in Fura-2-labeled platelets. Figure 3A shows typical responses following addition of 1- to 10- $\mu\text{M}$  GNF362 to Fura-2-labeled cells in the presence of 1 mM  $\text{Ca}^{2+}$  causing transient elevation of  $\text{Ca}^{2+}$  that peaked within 30 seconds and then returned to near basal levels within 5 minutes (maximal response seen between different platelet preparations ranged between 150 and nearly 400 nM but was transient and returned to near basal levels by 5 minutes).  $\text{Ca}^{2+}$  elevation by GNF362 correlated with the shape change response seen in washed platelets.  $\text{Ca}^{2+}$  elevation by GNF362 was also observed in platelets incubated with 0.1 mM EGTA to chelate extracellular  $\text{Ca}^{2+}$  and thus indicates an initial  $\text{Ca}^{2+}$  release from stores (results not shown). Again, this was transient and went back to near basal levels within 5 minutes. We tested for effects on agonist-induced  $\text{Ca}^{2+}$  elevation after 5-minute incubation of GNF362. The presence of 10  $\mu\text{M}$  GNF362 significantly enhanced the peak height of  $\text{Ca}^{2+}$  elevation seen with 0.12-U/mL thrombin (Figure 3B), with statistics shown as peak increase (nM  $\text{Ca}^{2+}$ ) above basal levels (Figure 3C;  $P = .003$ ). When GNF362 was tested at a concentration of 0.5  $\mu\text{M}$  that did not cause  $\text{Ca}^{2+}$  elevation by itself, there was still an enhancement of the  $\text{Ca}^{2+}$  response to agonists. Typically, Figure 3D-G shows that 0.5  $\mu\text{M}$  GNF362 enhanced the peak responses seen with 1  $\mu\text{M}$  U46619 and 10- $\mu\text{g}/\text{mL}$  collagen. To test if the presence of GNF362 would affect  $\text{IP}_3$  levels, we carried out preliminary studies measuring  $\text{IP}_3$  levels using an  $\text{IP}_3$ -ELISA kit as described in the Methods. Platelets resuspended at  $4 \times 10^8$  cells/mL and incubated at 37 °C with 10  $\mu\text{M}$  GNF362 for 1 minute increased basal levels of  $\text{IP}_3$  from  $151.7 \pm 10.9$  pg/mL to  $193.0 \pm 10.3$  pg/mL ( $n = 3$ ;  $P = .04$ ). This suggests that inhibition of ITPK by GNF362 may increase basal levels of  $\text{IP}_3$  contributing to the activation seen.

### 3.2 | $\text{IP}_4$ inhibits activation of saponin-permeabilized platelets

The product of ITPK ( $\text{IP}_4$ ) is water-soluble and not able to cross cell membranes. To test if it could exert actions on cell activation, we tested for effects on various activities measurable in saponin-permeabilized platelets. We have previously shown saponin at 13 to 15  $\mu\text{g}/\text{mL}$  to permeabilize washed platelets within 1 minute (as determined by release of adenine metabolites) and will cause a small

increase in light transmission as measured by aggregometry, representing ~12% to 16% aggregation over an 8-minute incubation [30]. We have also shown the nonhydrolyzable analog of GTP ( $\text{GTP}\gamma\text{S}$ ) and  $\text{IP}_3$  to further accelerate aggregation of saponin-treated platelets and induce thromboxane  $\text{B}_2$  formation and dense granule secretion [31,32].  $\text{GTP}\gamma\text{S}$  and  $\text{IP}_3$  are ineffective in intact cells, consistent with actions at intracellular sites. Therefore,  $\text{IP}_4$  was tested for effects on its own or if it altered  $\text{GTP}\gamma\text{S}$ - or  $\text{IP}_3$ -induced activation. Figure 4A shows that addition of 30  $\mu\text{M}$   $\text{IP}_4$  (tested range: 1-80  $\mu\text{M}$ ) to intact platelets caused no measurable effect on aggregation traces. Incubation of platelets with 14- $\mu\text{g}/\text{mL}$  saponin caused an approximately 10% to 15% increase of light transmission (% aggregation) over 8 minutes. The addition of 30  $\mu\text{M}$   $\text{IP}_4$  either 3 minutes before or 2 minutes after saponin addition had no further effect and mostly reduced the saponin effect by 2% to 3%, suggesting that it was not stimulatory. When tested with  $\text{GTP}\gamma\text{S}$ -induced aggregation,  $\text{IP}_4$  when added 3 minutes before saponin caused an inhibition of the  $\text{GTP}\gamma\text{S}$ -induced aggregation to the level seen with saponin alone ( $P = .0125$ ,  $n = 3$ ). Concentrations of  $\text{IP}_4$  at 0.1 to 1  $\mu\text{M}$  had little effect but those at  $\geq 10$   $\mu\text{M}$  showed significant inhibitory effects on aggregation (Figure 4B, C). The PI3K inhibitor LY294002 (tested at 25  $\mu\text{M}$  to inhibit all isoforms) also inhibited  $\text{GTP}\gamma\text{S}$ -induced response, suggesting that PI3K was important in this system. Similar inhibitory effects by  $\text{IP}_4$  were seen when  $\text{IP}_3$  was used to cause aggregation of permeabilized platelets (Figure 4D, E). No additive or synergistic effects between  $\text{IP}_4$  and  $\text{IP}_3$  were observed, suggesting distinct actions. The PI3K $\beta$  isoform specific inhibitor TGX221 was equally effective as LY294002 at inhibiting the  $\text{IP}_3$ -mediated aggregation response, suggesting that PI3K $\beta$  was the main isoform activated in this model.

The inhibitory effect of  $\text{IP}_4$  may be due to actions at multiple intracellular targets. As  $\text{IP}_4$  has the same headgroup as  $\text{PIP}_3$  and both LY294002 and TGX221 were inhibitory, we considered that it may target PI3K-dependent pathways. A commonly used measure of PI3K activity is measurement of AKT phosphorylation [24]. At concentrations that cause aggregation,  $\text{GTP}\gamma\text{S}$  induced the phosphorylation of AKT-Ser<sup>473</sup> as measured using Western blotting with a specific phospho-AKT-Ser<sup>473</sup> antibody (Figure 5A-C).  $\text{GTP}\gamma\text{S}$ -stimulated phosphorylation of AKT-Ser<sup>473</sup> was inhibited by LY294002 (25  $\mu\text{M}$ ;  $P = .0001$ ,  $n = 3$ ) and by 30  $\mu\text{M}$   $\text{IP}_4$  ( $P = .0001$ ,  $n = 4$  against 100  $\mu\text{M}$   $\text{GTP}\gamma\text{S}$ ).  $\text{IP}_4$  thus inhibited a PI3K effector activity in permeabilized platelets.

$\text{IP}_4$  is known to bind the Ras GTPase-activating protein RASA3 [19]. RASA3 is known to inactivate Rap1 by increasing the conversion of Rap1-GTP to Rap1-GDP [33,34]. We therefore examined activation of Rap1 with  $\text{GTP}\gamma\text{S}$  and tested to see if  $\text{IP}_4$  affected the Rap1-GTP status. Figure 6A-C shows that in saponin-permeabilized platelets,

(D) Dose-response relationship for GNF362 against thrombin, means  $\pm$  SEM ( $n = 3$ );  $P = .004$  for 0.5  $\mu\text{M}$  GNF362,  $P = .0001$  for 1  $\mu\text{M}$  GNF362, and  $P = .0004$  for 10  $\mu\text{M}$  GNF362. (F) At 0.1  $\mu\text{M}$  U46619,  $P = .0001$  ( $n = 4$ ). (G, H) Whole blood-induced thrombus formation on collagen-coated capillaries in the presence and absence of 10  $\mu\text{M}$  GNF362. Panel G represents typical confocal images of thrombi formed in collagen-coated capillaries for VC or + GNF362 (GNF); (H) values are means  $\pm$  SEM ( $n = 3$ ),  $P = .05$ . DMSO, dimethyl sulfoxide; VC, vehicle control.

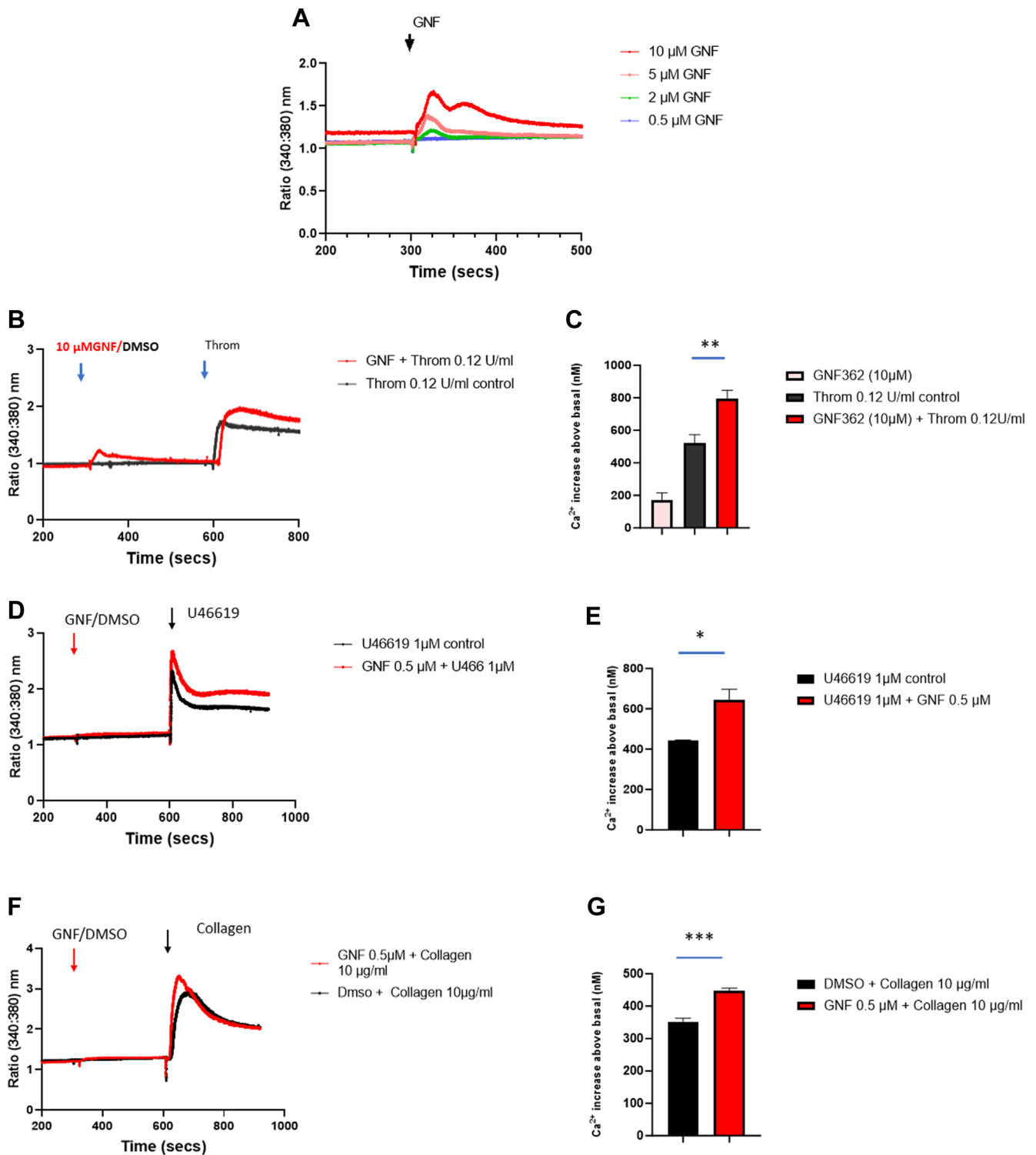


**FIGURE 3** GNF362 enhances Ca<sup>2+</sup> responses to agonists in Fura-2-labeled platelets. (A) Varying concentrations of GNF362 were added to Fura-2-loaded cells at indicated arrow, and recording representing ratio 340/380 nm excitation was made. Incubations contained 1 mM Ca<sup>2+</sup>. (B) GNF362 (GNF) or DMSO is added at 6 minutes followed by thrombin (0.12 U/mL) at 10 minutes. (C) Statistics for peak increases above basal of Ca<sup>2+</sup> (nM) for 0.12-U/mL thrombin vs 0.12-U/mL thrombin + 10  $\mu$ M GNF362 ( $P = .003$ ; values are means  $\pm$  SEM;  $n = 3$ ); Student's unpaired  $t$ -test used for all  $P$  values. (D) Ca<sup>2+</sup> responses for 1  $\mu$ M U46619 vs 1  $\mu$ M U46619 + 0.5  $\mu$ M GNF362. (E) Peak increases of Ca<sup>2+</sup> (nM) for panel D (means  $\pm$  SEM;  $n = 3$ ,  $P = .022$ ). (F) Ca<sup>2+</sup> responses for 10- $\mu$ g/mL collagen vs 10- $\mu$ g/mL collagen + 0.5  $\mu$ M GNF362. (G) Peak increases of Ca<sup>2+</sup> (nM) for panel F (means  $\pm$  SEM;  $n = 3$ ,  $P = .0003$ ). DMSO, dimethyl sulfoxide.

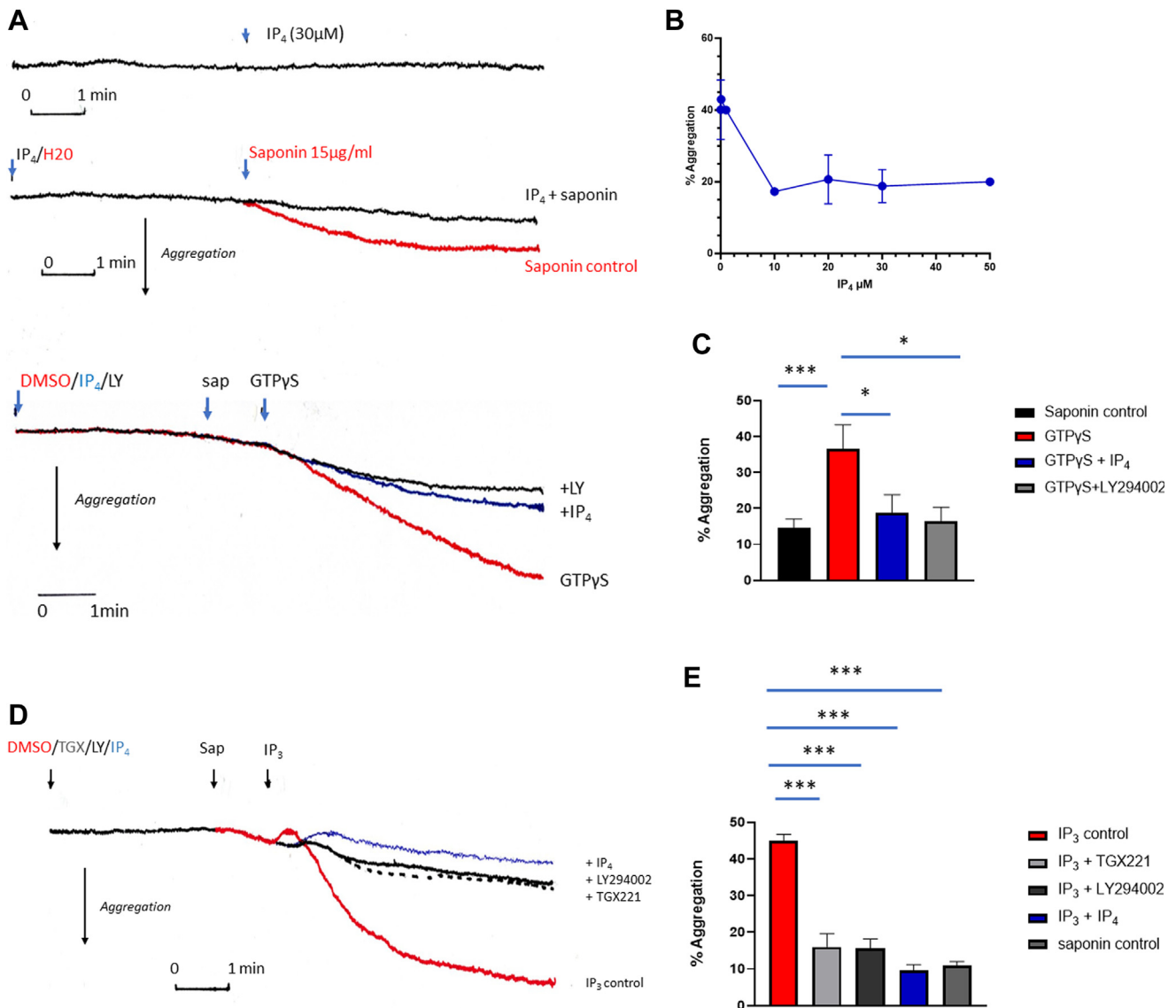


**FIGURE 4** IP<sub>4</sub> inhibits aggregation of saponin-permeabilized platelets. Platelets were resuspended in high K<sup>+</sup> medium (see Methods for details) and placed in aggregation cuvettes at 37 °C. After 3 minutes, equilibration reagents were added as indicated. (A) Top part: IP<sub>4</sub> (30 μM) alone; middle part: saponin (15 μg/mL, red trace) in the presence and absence of IP<sub>4</sub> (30 μM); and bottom part: saponin (sap; 15 μg/mL) + GTPγS (100 μM, red trace) in the presence of LY294002 (LY; 25 μM, black trace) or IP<sub>4</sub> (30 μM, blue trace). Saponin control left out for clarity. (B) Dose–response relationship for IP<sub>4</sub> inhibition of aggregation induced by GTPγS (means ± SEM; n = 3). (C) Effect of IP<sub>4</sub> (30 μM) and LY294002 (25 μM) on 100 μM GTPγS-induced aggregation of saponin-permeabilized platelets (means ± SEM, n = 3). *P* values calculated using Student’s unpaired *t*-test: *P* = .0009 for saponin control vs GTPγS; *P* = .0125 for GTPγS vs GTPγS + IP<sub>4</sub>; and *P* = .016 for GTPγS vs GTPγS + LY294002. (D) Effect of LY294002 (25 μM), TGX221 (10 μM), and IP<sub>4</sub> (30 μM) on 90 μM IP<sub>3</sub>-induced aggregation of saponin-permeabilized platelets. (E) Statistics of panel D: values are means ± SEM (n = 3)—*P* = .0002 for IP<sub>3</sub> vs IP<sub>3</sub> + TGX221; *P* = .0001 for IP<sub>3</sub> vs IP<sub>3</sub> + LY294002; *P* = .0001 for IP<sub>3</sub> vs IP<sub>3</sub> + IP<sub>4</sub>; and *P* = .0001 for IP<sub>3</sub> vs saponin control. IP<sub>3</sub>, inositol 1,4,5-trisphosphate; IP<sub>4</sub>, inositol 1,3,4,5-tetrakisphosphate.

GTPγS induces activation of Rap1 as estimated by pull-down assays using RalGDS-RBD beads. When tested for effects with IP<sub>4</sub> alone, there was no effect on Rap1-GTP levels, but at 30 μM, it caused a 27 % inhibition (*P* = .012) of 100 μM GTPγS-induced formation of Rap1-GTP. Under the same conditions, the PI3K inhibitor LY294002 had no significant effect on 100 μM GTPγS-induced Rap1-GTP formation. This suggested that GTPγS induced Rap1-GTP independently of PI3K activity. IP<sub>4</sub> may possibly act directly on RASA3, resulting in reduced Rap-1-GTP levels.

### 3.3 | IP<sub>4</sub> inhibits extraction of platelet PH domain proteins using PIP<sub>3</sub> beads

In order to understand the mechanism of inhibitory action of IP<sub>4</sub>, we sought to determine if IP<sub>4</sub> would displace PIP<sub>3</sub> from PH domains of known PIP<sub>3</sub> binding proteins. PIP<sub>3</sub>-coupled beads have been used to capture PIP<sub>3</sub> binding proteins from cellular lysates including platelets [35]. Therefore, platelet lysates were incubated with control or PIP<sub>3</sub> beads in the presence or absence of DiC8-PIP<sub>3</sub> or IP<sub>4</sub>. After binding,

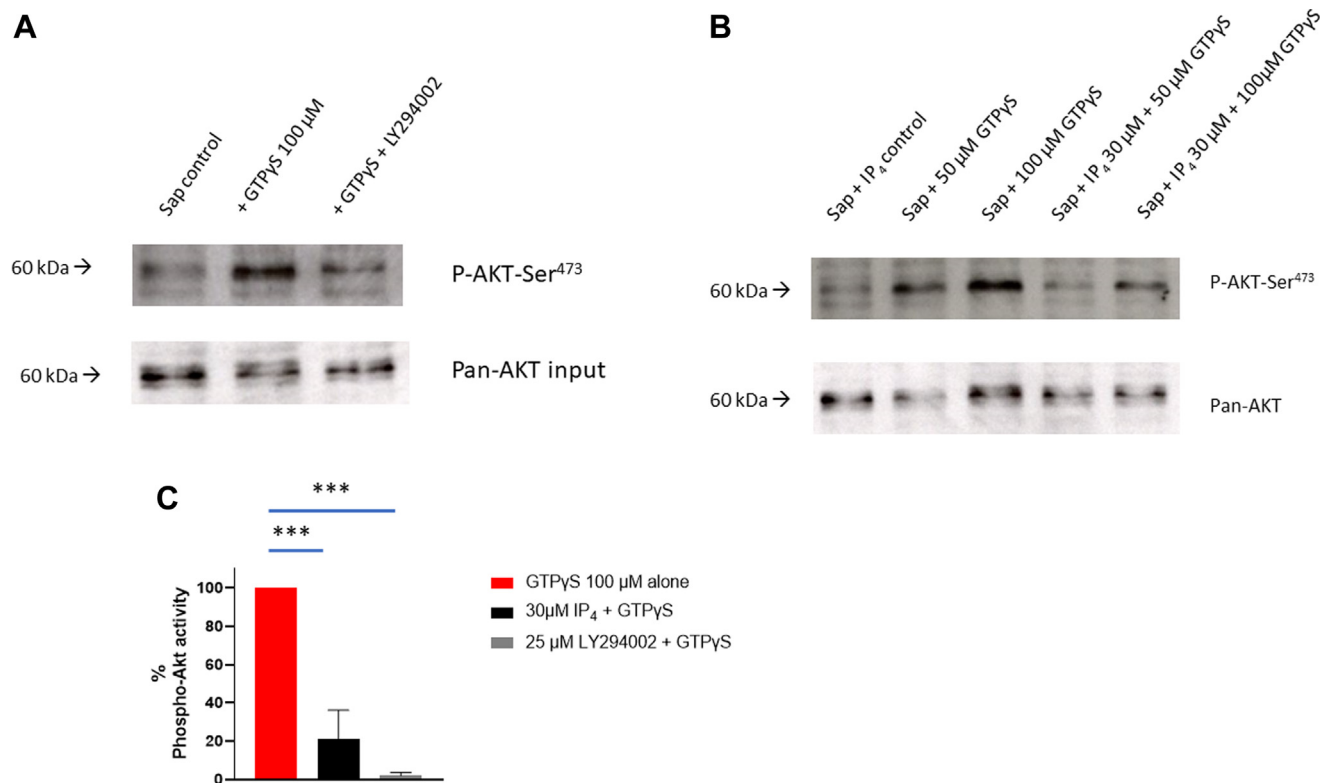


**FIGURE 5** IP<sub>4</sub> inhibits GTPγS-induced AKT-Ser<sup>473</sup> phosphorylation in saponin-permeabilized platelets. Experiments were carried out as in Figure 4. At the end of the incubations, cells were lysed with NP40 lysis buffer (see Methods for details). After centrifugation and addition of Laemmli buffer, the lysates were estimated for AKT-Ser<sup>473</sup> phosphorylation using phospho-AKT-Ser<sup>473</sup> antibody and total AKT (with pan-AKT antibody, depicting total input) by Western blotting. (A) LY294002 (25 μM) was tested against 100 μM GTPγS. (B) Fifty micromolar and 100 μM concentrations of GTPγS were tested against 30 μM IP<sub>4</sub>. (C) Statistics of 100 μM GTPγS vs 30 μM IP<sub>4</sub> and 25 μM LY294002 inhibition of AKT-Ser<sup>473</sup> phosphorylation; values are means ± SEM ( $n = 4$  for GTPγS,  $n = 4$  for GTPγS + IP<sub>4</sub>, and  $n = 3$  for GTPγS + LY294002). \*\*\* $P = .0001$  calculated using Student's unpaired  $t$ -test. IP<sub>4</sub>, inositol 1,3,4,5-tetrakisphosphate.

the beads were isolated and analyzed by Western blotting for the pull-down of PIP<sub>3</sub>-binding proteins. Figure 7A shows that RASA3 is efficiently extracted by PIP<sub>3</sub> beads and that this extraction was competed for by 40 μM DiC8-PIP<sub>3</sub> (Figure 7A [lanes 2 and 3]). Examination of the platelet lysate after PIP<sub>3</sub> bead incubation showed 87% reduction in RASA3 protein compared with control beads (compare lanes 7 and 8), confirming PIP<sub>3</sub>-mediated extraction. The inclusion of IP<sub>4</sub> potentially inhibited extraction of RASA3 by PIP<sub>3</sub> beads (lanes 4 and 5). Competition for PIP<sub>3</sub> binding to RASA3 was evident at 1 μM IP<sub>4</sub>, with increasing concentrations showing stronger displacement such that at 40 μM, there was >90% inhibition of RASA3 extraction on PIP<sub>3</sub> beads (statistics shown in Figure 7B). Under the same conditions, 40 μM IP<sub>3</sub> was without effect, indicating distinct actions of IP<sub>4</sub> compared to IP<sub>3</sub>. In a similar manner, IP<sub>4</sub> also reduced extraction of the PH domain-bearing tyrosine kinase BTK (Figure 7A, C). Compared to IP<sub>4</sub>, exogenously added DiC8-PIP<sub>3</sub> was marginally less potent at competing with PIP<sub>3</sub> beads. This may reflect the lack of intact membranes in the lysates with which this reagent will fuse as DiC8-PIP<sub>3</sub> is highly polarized and/or that IP<sub>4</sub> has a higher binding affinity. Our findings suggest IP<sub>4</sub> to strongly antagonize PI3K effectors to inhibit cell activation.

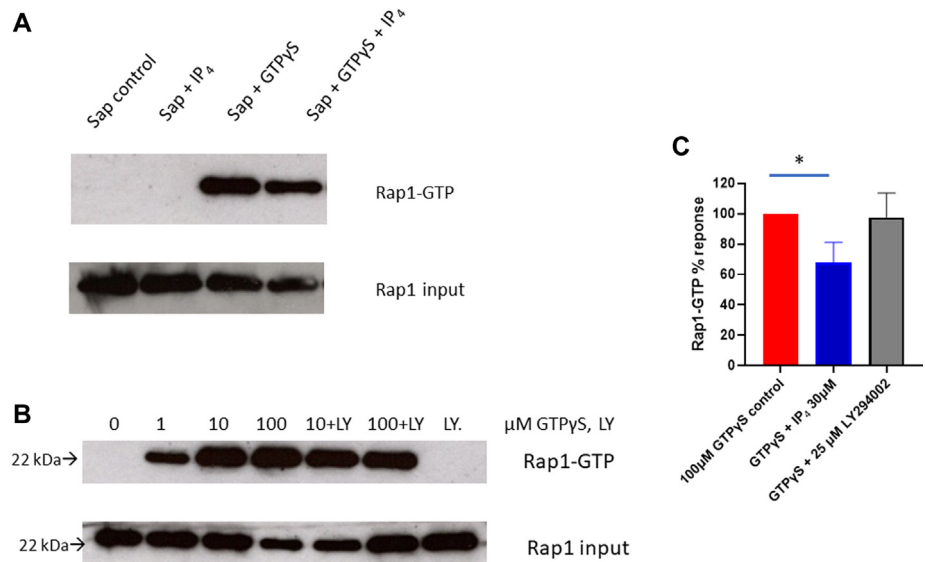
## 4 | DISCUSSION

This study identifies ITPK and IP<sub>4</sub> as negative regulators of platelet activation and represents a mechanism to finetune the activation process induced by all the agonists tested thus far. IP<sub>4</sub> formation is an ATP-requiring Ca<sup>2+</sup>-dependent pathway to metabolize the Ca<sup>2+</sup> mobilizing messenger IP<sub>3</sub> [11,36]. Since its discovery, various investigators have described possible functions for IP<sub>4</sub>, which included roles in Ca<sup>2+</sup> influx [12,13,23], Ca<sup>2+</sup> entry into the nucleus [37], cooperation at the level of the IP<sub>3</sub>R [38], and inhibition of the IP<sub>3</sub>-5'-phosphatase [15]. In contrast, negative roles for IP<sub>4</sub> in Ca<sup>2+</sup> entry have also been described in immune cells [17,39], including an inhibitory effect for IP<sub>4</sub> on the Orai1 channel [17] and a regulatory function for IP<sub>4</sub> in the PI3K pathway in reducing AKT phosphorylation in immune cells [20,21,26,40,41]. Thus, an established role for IP<sub>4</sub> in cell function is not present. Only recently have specific inhibitors of ITPK been described (such as GNF362), and their use suggest an antagonist role for IP<sub>4</sub> in PI3K-dependent effects [26,42]. We report here human platelets to express at least ITPKA and ITPKB [43], and the presence of GNF362 resulted in an enhancement of platelet aggregation and Ca<sup>2+</sup> elevation induced by all agonists tested and increased thrombus

**FIGURE 6** GTP $\gamma$ S stimulates Rap1-GTP formation in saponin-permeabilized platelets and the effect of IP $_4$ .

Experiments were carried out as in

Figures 4 and 5. Rap1-GTP was extracted from NP40 lysates using RalGDS-RBD beads and Rap1-GTP determined using Western blotting with anti-Rap1(A+B) antibody. Blots shown are typical of 3 experiments. Rap1 input was determined using aliquots of NP40 lysates. (A) Incubations were carried out for 5 minutes with 100  $\mu$ M GTP $\gamma$ S and 30  $\mu$ M IP $_4$ . (B) Varying concentrations of GTP $\gamma$ S in the presence and absence of 25  $\mu$ M LY294002 for 5 minutes. (C) Statistics of 30  $\mu$ M IP $_4$  or 25  $\mu$ M LY294002 effects on 100  $\mu$ M GTP $\gamma$ S-stimulated Rap1-GTP formation. Values are means  $\pm$  SEM ( $n = 5$  for GTP $\gamma$ S,  $n = 3$  for GTP $\gamma$ S + IP $_4$ , and  $n = 3$  for GTP $\gamma$ S + LY294002). \* $P = .012$ , Student's unpaired  $t$ -test. IP $_4$ , inositol 1,3,4,5-tetrakisphosphate.



formation on collagen-coated capillaries (Figures 1–3). There appears increased potency of the reagent in washed vs PRP or whole blood, and this may reflect some binding to plasma proteins. In washed platelet suspensions, GNF362 at 5 to 10  $\mu$ M also induced shape change and a transient increase of intracellular Ca $^{2+}$ . This is most likely due to inhibition of basal turnover of IP $_3$  to IP $_4$ , resulting in transiently higher IP $_3$  levels leading to Ca $^{2+}$  elevation and activation. This suggests that even though platelets express both ITPKs and IP $_3$  5-phosphatases to metabolize IP $_3$  [44], ITPK may be the preferred route for IP $_3$  metabolism. Our future studies will examine the kinetics of this pathway in detail.

Our studies on permeabilized platelets show IP $_4$  as an antagonist of PI3K effectors. We have previously shown IP $_3$  and GTP $\gamma$ S to accelerate aggregation in saponin-permeabilized platelets, which results from the release of Ca $^{2+}$  from intracellular stores, activation of G proteins, and formation of thromboxane A $_2$  [30–32]. Here, we report IP $_4$  to inhibit AKT phosphorylation and aggregation, and to a modest extent Rap1-GTP formation. GTP $\gamma$ S will activate G proteins by displacing the resting GDP bound to the GTP-bound states. Rap1 in the GTP-bound form is important for Talin-dependent activation of the  $\alpha$ IIb $\beta$ 3 integrin complex (inside-out signaling) that is essential for rapid platelet aggregation [45,46]. The effect of IP $_4$  on active Rap-1 was inhibitory, suggesting an action of either directly stimulating RASA3 or displacing any bound PIP $_3$  from RASA3, leading to a reduced level of RAP1-GTP. The modest inhibition is probably related to the relative nonhydrolysable nature of GTP $\gamma$ S acting directly on Rap1. GTP $\gamma$ S addition led to stimulation of the PI-3K $\beta$  isoform, as the phosphorylation of AKT was inhibited by both LY294002 and the  $\beta$ -isoform specific inhibitor TGX-221. The IP $_4$ -induced inhibition of AKT phosphorylation suggests that PI3K effectors are the targets of IP $_4$  action.

AKT itself is known to be stimulatory in platelet activation [47]; however, how it may be linked to integrins or other aspects of platelet activation still needs to be better understood.

To understand IP $_4$  actions further, we examined PIP $_3$  binding to RASA3 and BTK, which were both almost totally extracted by PIP $_3$  beads [35]. IP $_4$  potently displaced RASA3 and BTK from PIP $_3$  beads, antagonizing PIP $_3$  action. In our hands, extraction of AKT with PIP $_3$  beads was faint, which may reflect lower copy numbers in platelets than from the extraction of RASA3 or BTK, or the affinity of the antibody may not be sufficient and therefore accurate analysis was not possible (results not shown). PI3K effectors play important enhancement roles at different stages of signaling. For ITAM-linked receptors, PI3K is important in activating PLC $\gamma$ 2 via BTK [48]. Lack of BTK in human platelets results in decreased collagen-induced tyrosine phosphorylation of PLC $\gamma$ 2, Ca $^{2+}$  mobilization, and aggregation [49]. The inhibition of BTK by IP $_4$  corroborates the enhancement of collagen-induced effects in intact platelets by GNF362. Although BTK deficiency did not affect thrombin-induced responses in the study of Quek et al. [49], it is of interest that all PLC isoforms (except the  $\zeta$  form) utilized by GPCRs have PH domains and therefore a potential for modulation by phosphoinositides and IP $_4$  [50]. Further studies are required to examine if IP $_4$  affects PLC isoforms important for GPCR-linked receptors. In thymocytes notably, IP $_4$  has been reported to increase IL-2-stimulated T-cell kinase (ITK, another Tec kinase) activity that subsequently stimulates PLC $\gamma$ 1 [51]. ITK has not been shown to be present in platelets, so if this reflects a cell-specific activity remains to be clarified. RASA3 is suggested to have a prominent role in inactivating Rap1, and its inhibition by the P2Y $_{12}$ R-PI3K-dependent or P2Y $_{12}$ R-PI3K-independent pathway is considered central to the sustained activation of Rap1 and stable integrin-dependent

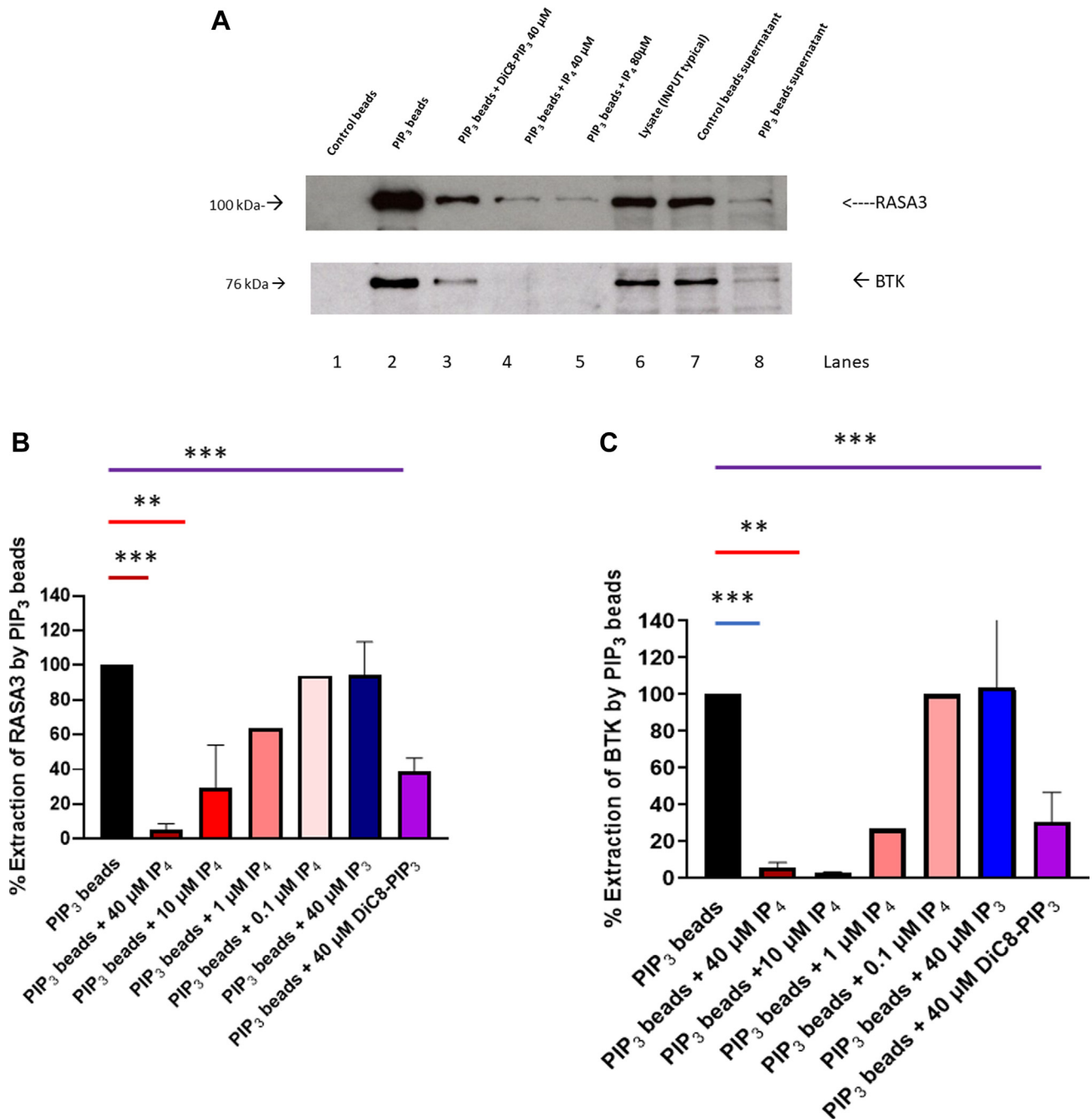


**FIGURE 7** Effect of IP<sub>4</sub> on extraction of RASA3 and BTK from NP40 platelet lysates by PIP<sub>3</sub> beads. Resting platelet lysates were incubated with either control beads or PIP<sub>3</sub> beads with or without exogenous inositol lipids and extracted, and proteins were detected by Western blotting. (A) Top: detection of RASA3; bottom: detection of BTK. Lysates were incubated with control beads (lane 1), PIP<sub>3</sub> beads (lane 2), PIP<sub>3</sub> beads + 40 μM DiC8-PIP<sub>3</sub> (lane 3), PIP<sub>3</sub> beads + 40 μM IP<sub>4</sub> (lane 4), PIP<sub>3</sub> beads + 80 μM IP<sub>4</sub> (lane 5), lysate (1/40 input of protein for each incubation, lane 6), post control bead lysate supernatant (1/40 of total, lane 7), and post PIP<sub>3</sub> beads supernatant (1/40 of total, lane 8). Images are typical of 3 different experiments. (B) Effect of varying doses of IP<sub>4</sub>, IP<sub>3</sub>, and DiC8-PIP<sub>3</sub> on RASA3 extraction with PIP<sub>3</sub> beads and (C) the same for BTK. Values are means ± SEM (n = 4); \*\*P = .0019 and \*\*\*P = .0001 calculated using Student's unpaired t-test. BTK, Bruton's tyrosine kinase; IP<sub>3</sub>, inositol 1,4,5-trisphosphate; IP<sub>4</sub>, inositol 1,3,4,5-tetrakisphosphate; PIP<sub>3</sub>, phosphatidylinositol 3,4,5-trisphosphate.

aggregation [33,34,52,53]. However, there has been to date no direct demonstration that PIP<sub>3</sub> inhibits RASA3. With most PI3K effectors, the binding of PIP<sub>3</sub> would result in activation of downstream targets (eg, with AKT) rather than inhibition (as proposed with RASA3), and therefore, this mechanism requires further elucidation. In intact

platelets, exogenous addition of DiC8-PIP<sub>3</sub> will stimulate Ca<sup>2+</sup> elevation transiently, increase thromboxane production, and stimulate AKT phosphorylation and aggregation [24]. However, in the saponin permeabilization model, addition of DiC8-PIP<sub>3</sub> has thus far been ineffective and did not affect GTPγS-stimulated Rap1-GTP formation

### Possible targets of IP<sub>4</sub> action in platelet signalling

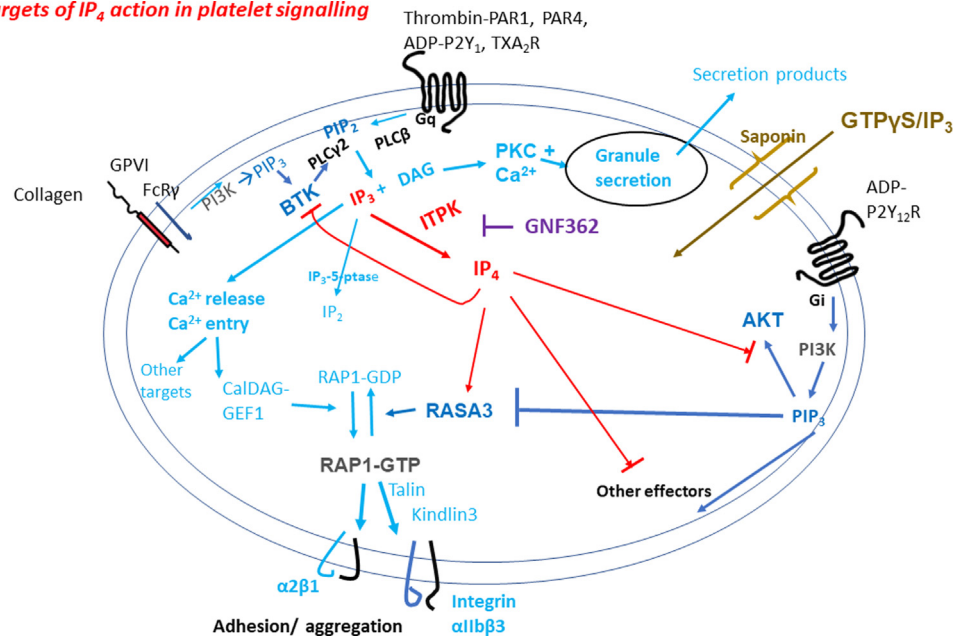


**FIGURE 8** Possible targets of IP<sub>4</sub> action in platelet signaling. G-protein-linked receptor agonists (such as thrombin, ADP, and thromboxane A<sub>2</sub>) and ITAM-linked agonist (such as collagen) activate PLCβ and PLCγ2, respectively. The resulting IP<sub>3</sub> and DAG elevate Ca<sup>2+</sup> and activate PKC. The elevated Ca<sup>2+</sup> activates many Ca<sup>2+</sup>-driven processes including CalDAG-GEF1 to promote Rap1-GTP formation, which promotes Talin to activate integrins such as αIIbβ<sub>3</sub>. IP<sub>3</sub> can be metabolized to IP<sub>4</sub> by ITPK or to IP<sub>2</sub> via IP<sub>3</sub> 5-phosphatase. PI3K can be activated as a consequence of ITAM signaling, stimulating BTK and PLCγ2. Additionally, G-protein-linked receptors, principally ADP-P2Y<sub>12</sub>R, can stimulate PI3K, resulting in activation of effectors such as AKT, and proposed RASA3 inhibition. In saponin-permeabilized platelets, GTPγS/IP<sub>3</sub> can access the intracellular space and activate G proteins, including Rap1, Ca<sup>2+</sup> elevation, and PI3K activation. IP<sub>4</sub> is suggested to antagonize PI3K effectors by binding to and/or displacing PIP<sub>3</sub> from PH domains. RASA3, BTK, AKT, and other PH domain containing proteins represent potent IP<sub>4</sub> targets. GNF362 inhibits ITPK, resulting in decreased IP<sub>4</sub>, increased IP<sub>3</sub> levels, and an enhancement of agonist function. For further details, see Discussion. DAG, 1,2-diacylglycerol; IP<sub>3</sub>, inositol 1,4,5-trisphosphate; IP<sub>4</sub>, inositol 1,3,4,5-tetrakisphosphate; ITPK, inositol 1,4,5-trisphosphate 3-kinase.

(results not shown). It has been suggested recently that PI3K stimulated production of PIP<sub>3</sub> and that its binding to RASA3 may restrict RASA3 to the membrane and limit its ability to inactivate Rap1 [54]. IP<sub>4</sub>, which is generated in the cytosol, will be freely available to act on RASA3 to control Rap1.

In summary, our studies suggest ITPK and IP<sub>4</sub> to be important negative regulators of platelet activation by controlling levels of IP<sub>3</sub> and antagonizing PIP<sub>3</sub> actions. Figure 8 outlines possible mechanisms for IP<sub>4</sub> with actions at the level of RASA3, BTK, and AKT. We predict many more PH domain proteins to be affected by IP<sub>4</sub> and further studies are underway to elucidate their importance. The increased synthesis or the development of cell-permeable mimetics of IP<sub>4</sub> may represent useful strategies for antithrombotic therapeutics.

### AUTHOR CONTRIBUTIONS

K.S.A. designed the project, raised funding, performed experiments, and wrote the manuscript. S.K. performed experiments. J.M.G. contributed to experimental design and writing of the manuscript. S.D.B. contributed to raising funds and writing of the manuscript. All authors approved the final manuscript.

### FUNDING

This work was supported by grants from the British Heart Foundation (PG/19/72/34642 [to K.S.A. and S.D.B.] and RG/20/7/34866 [to J.M.G.]). S.K. is funded by Quercis Pharma.

### RELATIONSHIP DISCLOSURE

There are no competing interests to disclose.

### TWITTER

Jonathan M. Gibbins  @RdgPlateletLabs

### REFERENCES

- [1] Varga-Szabo D, Braun A, Kleinschnitz C, Bender M, Pleines I, Pham M, et al. The calcium sensor STIM1 is an essential mediator of arterial thrombosis and ischemic brain infarction. *J Exp Med*. 2008;205:1583–91.
- [2] Braun A, Varga-Szabo D, Kleinschnitz C, Pleines I, Bender M, Austinat M, et al. Orai1 (CRACM1) is the platelet SOC channel and essential for pathological thrombus formation. *Blood*. 2009;113:2056–63.
- [3] Volz J, Mammadova-Bach E, Gil-Pulido J, Nandigama R, Remer K, Sorokin L, et al. Inhibition of platelet GPVI induces intratumor

- hemorrhage and increases efficacy of chemotherapy in mice. *Blood*. 2019;133:2696–706.
- [4] Authi KS. Orai1: a channel to safer antithrombotic therapy. *Blood*. 2009;113:1872–3.
- [5] Mammadova-Bach E, Nagy M, Heemskerk JWM, Nieswandt B, Braun A. Store-operated calcium entry in thrombosis and thromboinflammation. *Cell Calcium*. 2019;77:39–48.
- [6] Varga-Szabo D, Braun A, Nieswandt B. Calcium signaling in platelets. *J Thromb Haemost*. 2009;7:1057–66.
- [7] Brehm MA, Klemm U, Rehbach C, Erdmann N, Kolšek K, Lin H, et al. Inositol hexakisphosphate increases the size of platelet aggregates. *Biochem Pharmacol*. 2019;161:14–25.
- [8] Guillemette G, Balla T, Baukal AJ, Catt KJ. Metabolism of inositol 1,4,5-trisphosphate to higher inositol phosphates in bovine adrenal cytosol. *Am J Hypertens*. 1989;2:387–94.
- [9] Daniel JL, Dangelmaier CA, Smith JB. Calcium modulates the generation of inositol 1,3,4-trisphosphate in human platelets by the activation of inositol 1,4,5-trisphosphate 3-kinase. *Biochem J*. 1988;253:789–94.
- [10] Ribes A, Oprescu A, Viaud J, Hnia K, Chicanne G, Xuereb JM, et al. Phosphoinositide 3-kinases in platelets, thrombosis and therapeutics. *Biochem J*. 2020;477:4327–42.
- [11] Irvine RF, Letcher AJ, Heslop JP, Berridge MJ. The inositol tris/tetrakisphosphate pathway—demonstration of Ins(1,4,5)P<sub>3</sub> 3-kinase activity in animal tissues. *Nature*. 1986;320:631–4.
- [12] Irvine RF, Moor RM. Micro-injection of inositol 1,3,4,5-tetrakisphosphate activates sea urchin eggs by a mechanism dependent on external Ca<sup>2+</sup>. *Biochem J*. 1986;240:917–20.
- [13] Lückhoff A, Clapham DE. Inositol 1,3,4,5-tetrakisphosphate activates an endothelial Ca<sup>2+</sup>-permeable channel. *Nature*. 1992;355:356–8.
- [14] Changya L, Gallacher DV, Irvine RF, Potter BV, Petersen OH. Inositol 1,3,4,5-tetrakisphosphate is essential for sustained activation of the Ca<sup>2+</sup>-dependent K<sup>+</sup> current in single internally perfused mouse lacrimal acinar cells. *J Membr Biol*. 1989;109:85–93.
- [15] Hermosura MC, Takeuchi H, Fleig A, Riley AM, Potter BVL, Hirata M, et al. InsP<sub>4</sub> facilitates store-operated calcium influx by inhibition of InsP<sub>3</sub> 5-phosphatase. *Nature*. 2000;408:735–40.
- [16] Marongiu L, Mingozzi F, Cigni C, Marzi R, Di Gioia M, Garrè M, et al. Inositol 1,4,5-trisphosphate 3-kinase B promotes Ca<sup>2+</sup> mobilization and the inflammatory activity of dendritic cells. *Sci Signal*. 2021;14:eaz2120. <https://doi.org/10.1126/scisignal.aaz2120>
- [17] Miller AT, Dahlberg C, Sandberg ML, Wen BG, Beisner DR, Hoerter JA, et al. Inhibition of the inositol kinase Itpkb augments calcium signaling in lymphocytes and reveals a novel strategy to treat autoimmune disease. *PLoS One*. 2015;10:e0131071. <https://doi.org/10.1371/journal.pone.0131071>
- [18] Baraldi E, Djjinovic Carugo K, Hyvönen M, Surdo PL, Riley AM, Potter BV, et al. Structure of the PH domain from Bruton's tyrosine kinase in complex with inositol 1,3,4,5-tetrakisphosphate. *Structure*. 1999;7:449–60.
- [19] Cullen PJ, Hsuan JJ, Truong O, Letcher AJ, Jackson TR, Dawson AP, et al. Identification of a specific Ins(1,3,4,5)P<sub>4</sub>-binding protein as a member of the GAP1 family. *Nature*. 1995;376:527–30.
- [20] Sauer K, Park E, Siegemund S, French AR, Wahle JA, Sternberg L, et al. Inositol tetrakisphosphate limits NK cell effector functions by controlling PI3K signaling. *Blood*. 2013;121:286–97.
- [21] Siegemund S, Rigaud S, Conche C, Broaten B, Schaffer L, Westernberg L, et al. IP<sub>3</sub> 3-kinase B controls hematopoietic stem cell homeostasis and prevents lethal hematopoietic failure in mice. *Blood*. 2015;125:2786–97.
- [22] O'Rourke F, Matthews E, Feinstein MB. Isolation of InsP<sub>4</sub> and InsP<sub>6</sub> binding proteins from human platelets: InsP<sub>4</sub> promotes Ca<sup>2+</sup> efflux from inside-out plasma membrane vesicles containing 104 kDa GAP1IP<sub>4</sub>BP protein. *Biochem J*. 1996;315:1027–34.
- [23] El-Daher SS, Patel Y, Siddiqua A, Hassock S, Edmunds S, Maddison B, et al. Distinct localization and function of 1<sup>,4,5</sup>IP<sub>3</sub> receptor subtypes and the 1<sup>,3,4,5</sup>IP<sub>4</sub> receptor GAP1<sup>IP<sub>4</sub>BP</sup> in highly purified human platelet membranes. *Blood*. 2000;95:3412–22.
- [24] Kassouf N, Ambily A, Watson S, Hassock S, Authi HS, Srivastava S, et al. Phosphatidylinositol-3,4,5-trisphosphate stimulates Ca<sup>2+</sup> elevation and Akt phosphorylation to constitute a major mechanism of thromboxane A<sub>2</sub> formation in human platelets. *Cell Signal*. 2015;27:1488–98.
- [25] Kwon Y, Hofmann T, Montell C. Integration of phosphoinositide- and calmodulin-mediated regulation of TRPC6. *Mol Cell*. 2007;25:491–503.
- [26] Thangavelu G, Du J, Paz KG, Loschi M, Zaiken MC, Flynn R, et al. Inhibition of inositol kinase B controls acute and chronic graft-versus-host disease. *Blood*. 2020;135:28–40.
- [27] Gryniewicz G, Poenie M, Tsien RY. A new generation of Ca<sup>2+</sup> indicators with greatly improved fluorescence properties. *J Biol Chem*. 1985;260:3440–50.
- [28] Sage SO. Use of fluorescent indicators to measure intracellular Ca<sup>2+</sup> and other ions. In: Watson SP, Authi KS, eds. *Platelets: a practical approach*. Oxford: Oxford University Press; 1996:67–90.
- [29] Ambily A, Kaiser WJ, Pierro C, Chamberlain EV, Li Z, Jones CI, et al. The role of plasma membrane STIM1 and Ca<sup>2+</sup> entry in platelet aggregation. STIM1 binds to novel proteins in human platelets. *Cell Signal*. 2014;26:502–11.
- [30] Authi KS, Evenden BJ, Crawford N. Metabolic and functional consequences of introducing inositol 1,4,5-trisphosphate into saponin-permeabilized human platelets. *Biochem J*. 1986;233:707–18.
- [31] Authi KS, Rao GH, Evenden BJ, Crawford N. Action of guanosine 5'-[beta-thio]diphosphate on thrombin-induced activation and Ca<sup>2+</sup> mobilization in saponin-permeabilized and intact human platelets. *Biochem J*. 1988;255:885–93.
- [32] Authi KS, Hornby EJ, Evenden BJ, Crawford N. Inositol 1,4,5-trisphosphate (IP<sub>3</sub>) induced rapid formation of thromboxane B<sub>2</sub> in saponin-permeabilised human platelets: mechanism of IP<sub>3</sub> action. *FEBS Lett*. 1987;213:95–101.
- [33] Stefanini L, Paul DS, Robledo RF, Chan ER, Getz TM, Campbell RA, et al. RASA3 is a critical inhibitor of RAP1-dependent platelet activation. *J Clin Invest*. 2015;125:1419–32.
- [34] Battram AM, Durrant TN, Agbani EO, Heesom KJ, Paul DS, Piatt R, et al. The phosphatidylinositol 3,4,5-trisphosphate (PI(3,4,5)P<sub>3</sub>) binder Rasa3 regulates phosphoinositide 3-kinase (PI3K)-dependent integrin α<sub>IIb</sub>β<sub>3</sub> outside-in signaling. *J Biol Chem*. 2017;292:1691–704.
- [35] Durrant TN, Hutchinson JL, Heesom KJ, Anderson KE, Stephens LR, Hawkins PT, et al. In-depth PtdIns(3,4,5)P<sub>3</sub> signalosome analysis identifies DAPP1 as a negative regulator of GPVI-driven platelet function. *Blood Adv*. 2017;1:918–32.
- [36] Batty IR, Nahorski SR, Irvine RF. Rapid formation of inositol 1,3,4,5-tetrakisphosphate following muscarinic receptor stimulation of rat cerebral cortical slices. *Biochem J*. 1985;232:211–5.
- [37] Mishra OP, Delivoria-Papadopoulos M. Inositol tetrakisphosphate (IP<sub>4</sub>)- and inositol triphosphate (IP<sub>3</sub>)-dependent Ca<sup>2+</sup> influx in cortical neuronal nuclei of newborn piglets following graded hypoxia. *Neurochem Res*. 2004;29:391–6.
- [38] Wilcox RA, Challiss RA, Liu C, Potter BV, Nahorski SR. Inositol-1,3,4,5-tetrakisphosphate induces calcium mobilization via the inositol-1,4,5-trisphosphate receptor in SH-SY5Y neuroblastoma cells. *Mol Pharmacol*. 1993;44:810–7.
- [39] Miller AT, Sandberg M, Huang YH, Young M, Sutton S, Sauer K, et al. Production of Ins(1,3,4,5)P<sub>4</sub> mediated by the kinase Itpkb inhibits store-operated calcium channels and regulates B cell selection and activation. *Nat Immunol*. 2007;8:514–21.
- [40] Jia Y, Subramanian KK, Erneux C, Pouillon V, Hattori H, Jo H, You J, et al. Inositol 1,3,4,5-tetrakisphosphate negatively regulates phosphatidylinositol-3,4,5-trisphosphate signaling in neutrophils. *Immunity*. 2007;27:453–67.

- [41] Westernberg L, Conche C, Huang YH, Rigaud S, Deng Y, Siegemund S, et al. Non-canonical antagonism of PI3K by the kinase Itpkb delays thymocyte beta-selection and renders it Notch-dependent. *eLife*. 2016;5:e10786. <https://doi.org/10.7554/elife.10786>
- [42] Schröder D, Tödter K, Gonzalez B, Franco-Echevarría E, Rohaly G, Blecher C, et al. The new InsP3Kinase inhibitor BIP-4 is competitive to InsP3 and blocks proliferation and adhesion of lung cancer cells. *Biochem Pharmacol*. 2015;96:143–50.
- [43] Communi D, Vanweyenberg V, Erneux C. Purification and biochemical properties of a high-molecular-mass inositol 1,4,5-trisphosphate 3-kinase isoenzyme in human platelets. *Biochem J*. 1994;298:669–73.
- [44] Burkhart JM, Vaudel M, Gambaryan S, Radau S, Walter U, Martens L, et al. The first comprehensive and quantitative analysis of human platelet protein composition allows the comparative analysis of structural and functional pathways. *Blood*. 2012;120:e73–82.
- [45] Lagarrigue F, Paul DS, Gingras AR, Valadez AJ, Sun H, Lin J, et al. Talin-1 is the principal platelet Rap1 effector of integrin activation. *Blood*. 2020;136:1180–90.
- [46] Gingras AR, Lagarrigue F, Cuevas MN, Valadez AJ, Zorovich M, McLaughlin W, et al. Rap1 binding and a lipid-dependent helix in talin F1 domain promote integrin activation in tandem. *J Cell Biol*. 2019;218:1799–809.
- [47] Woulfe DS. Akt signaling in platelets and thrombosis. *Expert Rev Hematol*. 2010;3:81–91.
- [48] Watson SP, Auger JM, McCarty OJ, Pearce AC. GPVI and integrin  $\alpha\text{IIb}\beta\text{3}$  signaling in platelets. *J Thromb Haemost*. 2005;3:1752–62.
- [49] Quek LS, Bolen J, Watson SP. A role for Bruton's tyrosine kinase (Btk) in platelet activation by collagen. *Curr Biol*. 1998;8:1137–40.
- [50] Katan M, Cockcroft S. Phosphatidylinositol(4,5)bisphosphate: diverse functions at the plasma membrane. *Essays Biochem*. 2020;64:513–31.
- [51] Huang YH, Grasis JA, Miller AT, Xu R, Soonthornvacharin S, Andreotti AH, et al. Positive regulation of ITK PH domain function by soluble IP4. *Science*. 2007;316:886–9.
- [52] Stefanini L, Lee RH, Paul DS, O'Shaughnessy EC, Ghalloussi D, Jones CI, et al. Functional redundancy between RAP1 isoforms in murine platelet production and function. *Blood*. 2018;132:1951–62.
- [53] Dangelmaier C, Kunapuli SP. Evidence for a PI3-kinase independent pathway in the regulation of Rap1b activation downstream of the P2Y12 receptor in platelets. *Platelets*. 2022;33:1301–6.
- [54] Johansen KH, Golec DP, Huang B, Park C, Thomsen JH, Preite S, et al. A CRISPR screen targeting PI3K effectors identifies RASA3 as a negative regulator of LFA-1-mediated adhesion in T cells. *Sci Signal*. 2022;15:eab9169. <https://doi.org/10.1126/scisignal.abl9169>